Pergamon

0094-114X(94)00048-4

Mech. Mach. Theory Vol. 30, No. 3, pp. 323–339, 1995

0094-114X/95 $9.50 + 0.00

DYNAMIC FORCE TRANSMISSIBILITY IN HELICAL GEAR PAIRS

G. WESLEY BLANKENSHIP†
General Motors Corporation, Powertrain Division, 37350 Ecorse Road, Romulus, MI 48174-1376, U.S.A.

RAJENDRA SINGH
The Ohio State University, Department of Mechanical Engineering, 206 West Eighteenth Avenue, Columbus, OH 43210-1107, U.S.A.

(Received 15 October 1993; in revised form 15 July 1994; received for publication 1 September 1994)

Abstract—A new model is developed that describes mesh force transmissibility in a helical gear pair. New spectral stiffness and transmissibility matrices are developed, based on linear theory, which completely characterize the steady state forced response of a helical gear pair. New modal rating indices are also developed which can be used to rank order the importance of gear pair modes excited by various types of transmission error displacement excitations and to quantify gear mesh normal force and moment coupling. This study suggests that additional DOF must be included in the gear mesh interface model in those geared system analyses which attempt to predict structure borne noise and casing vibration associated with power transmission systems.

1. INTRODUCTION

In the dynamic analysis of geared power transmission systems which attempt to predict casing vibration and structure borne noise directly from vibratory source information, the corresponding gear pair models must describe not only vibratory excitation due to gear manufacturing errors and gear mesh stiffness variation but the transmission of external forces and moments via the gear mesh interface as well [1–3]. This latter issue has been largely ignored by prior gear researchers who have developed analytical gear pair models [4–10] or conducted experimental investigations [11–14]. These gear pair analyses have concentrated primarily on the prediction of vibratory gear motions and dynamic tooth stresses arising from gear manufacturing errors and mesh stiffness variation with an emphasis on minimization of gear source terms such as dynamic mesh force or transmission error displacement excitation [1]. However, several structural dynamics and finite element researchers have approached the geared system problem from the viewpoint of frequency response functions and system modes without performing detailed analyses of the gear mesh interface [2, 3]. The emphasis here has been on the identification of structural mesh force transmission paths and housing radiation efficiency. When both approaches are viewed together as elements of an overall dynamic system analysis, several issues emerge. These include the formal definition of mesh force transmissibility terms, identification or ranking of important system modes and the truncation of gear mesh interface degrees-of-freedom (DOF) in modal analyses of specific classes of geared systems.

In order to address such research issues, the authors have recently developed a generalized six DOF helical gear pair model [15]. In this study, the gear pair model is reduced to various simplified linear forms and dynamic analyses are performed which clearly illustrate that the transmission of forces and moments, other than conventional line-of-action mesh force and torsional moment, via the gear mesh interface is indeed significant. This study further suggests that additional DOF must be included in the gear mesh interface model when non-conventional forces and moments are of interest. The current paper is an extension of Ref. [15] as new spectral mesh stiffness and transmissibility matrices are introduced, based on the linear theory, which can be used to

†To whom all correspondence should be addressed.

characterize the generation and transmission of forces and moments within the gear mesh interface. New modal rating indices are also introduced which can be used to rank order the importance of gear pair modes excited by various types of transmission error displacement excitations and to quantify gear mesh normal force and moment coupling.

1.1. Scope and assumptions

The aim of this study is to illustrate the importance of off-line-of-action force transmissibility associated with a single stage helical gear pair operating under steady-state conditions. A reduced form of the new gear mesh interface dynamic model developed recently by Blankenship and Singh [15] is used in conjunction with a 10 DOF linear time-invariant (LTI) system model. Several assumptions are implicit to this analysis. Translations of the gear body normal to the line-of-action are neglected. The gear pair is assumed to be operating at speeds sufficiently low so that gyroscopic moments can be neglected. Further, no misalignments or mass unbalances are considered. Loss of tooth contact due to gear backlash phenomenon and any other nonlinear effects are also ignored. Gear bodies are assumed to be rigid except for the elastic compliance of meshing gear teeth. Only time-invariant gear mesh stiffness, damping and inertial properties are considered. Inertial effects of shafting and bearings are neglected; although energy equivalent bearing stiffness and damping matrices are assumed in order to account for elastic deformations and dissipative effects associated with these elements.

2. DYNAMIC MODEL

An external helical involute gear pair ij is shown in Fig. 1. Each gear i is represented by a base cylinder of radius a^i and width $2b^i$. The origins O^i of two non-rotating reference frames (X^i, Y^i, Z^i) and (X^j, Y^j, Z^j) are located on the respective gear bodies i and j as shown such that the orientation of either frame remains parallel to the inertial frame. Intended rotation of each gear is about its Z^i axis and the Y^i axes are chosen to lie in the theoretical plane-of-action. Any out-of-plane motions in the X-direction are neglected. Accordingly, the displacement of each gear i from its ideal angular motion $\Omega^i t$ is described by the generalized coordinate vector $\mathbf{x}^i(t) = \{y^i(t)\ z^i(t)\ \theta_x^i(t)\ \theta_y^i(t)\ \theta_z^i(t)\}^T$; these vibratory motions are labeled in Fig. 1. Here Ω^i is the mean rotational velocity of gear i about

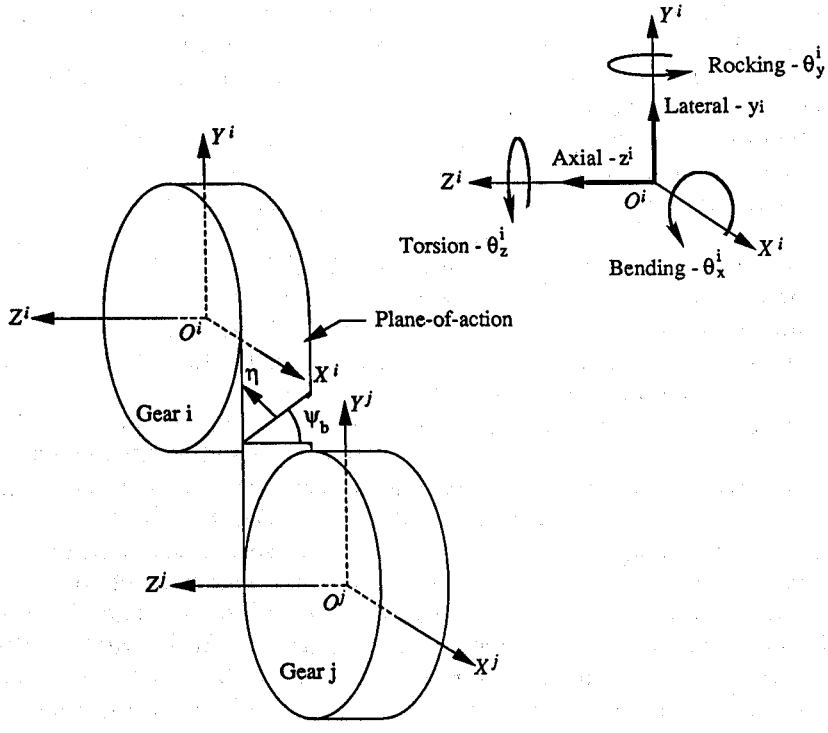

Fig. 1. Physical model: helical gear pair model showing plane-of-action, tooth normal vector η and vibratory motions.

the Z^i axis. Angular velocities Ω^i and Ω^j are related by the kinematic constraint equation $\Omega^i = \lambda^{ij}\Omega^j$ where λ^{ij} is the gear ratio. The mass centroid of each gear is assumed to lie along the Z^i axis although it does not necessarily coincide with the geometric origin O^i; hence, rotational mass unbalance is not considered in the present formulation. The 10 DOF dynamic equation of motion for gear pair ij written in terms of generalized translational coordinates $\mathbf{q}^i(t) = \mathbf{D}^i\mathbf{x}^i(t)$ and $\mathbf{q}^j(t) = \mathbf{D}^j\mathbf{x}^j(t)$ is given by

$$\begin{pmatrix} [\mathbf{D}^i]^{-1}\mathbf{M}^i[\mathbf{D}^i]^{-1} & \mathbf{O} \\ \mathbf{O} & [\mathbf{D}^j]^{-1}\mathbf{M}^j[\mathbf{D}^j]^{-1} \end{pmatrix} \begin{Bmatrix} \ddot{\mathbf{q}}^i(t) \\ \ddot{\mathbf{q}}^j(t) \end{Bmatrix} + \mathbf{C} \begin{Bmatrix} \dot{\mathbf{q}}^i(t) \\ \dot{\mathbf{q}}^j(t) \end{Bmatrix} + \mathbf{K} \begin{Bmatrix} \mathbf{q}^i(t) \\ \mathbf{q}^j(t) \end{Bmatrix} = \begin{Bmatrix} \mathbf{Q}^i(t) \\ \mathbf{Q}^j(t) \end{Bmatrix}; \tag{1}$$

where $(\dot{})$ denotes differentiation with respect to time and $\mathbf{D}^i$ is a diagonal transformation matrix of dimension five given by

$$\mathbf{D}^i = \text{diag}[1 \quad 1 \quad b^i \quad a^i \quad a^i]. \tag{2}$$

The diagonal mass matrix $\mathbf{M}^i$ associated with each gear i is given by

$$\mathbf{M}^i = \text{diag}[m^i \quad m^i \quad I_x^i \quad I_y^i \quad I_z^i]; \tag{3}$$

where I_x^i, I_y^i and I_z^i are the polar mass moments of inertia of gear i about the X^i, Y^i and Z^i gear body axes, respectively, and m^i is the mass of gear i. The system stiffness matrix is given by

$$\mathbf{K} = \begin{bmatrix} \hat{\mathbf{K}}_M^{ij} & \mathbf{P}\hat{\mathbf{K}}_M^{ij} \\ \mathbf{P}\hat{\mathbf{K}}_M^{ji} & \hat{\mathbf{K}}_M^{ji} \end{bmatrix} + \begin{bmatrix} [\mathbf{D}^i]^{-1}\mathbf{K}_B^i[\mathbf{D}^i]^{-1} & \mathbf{O} \\ \mathbf{O} & [\mathbf{D}^j]^{-1}\mathbf{K}_B^j[\mathbf{D}^j]^{-1} \end{bmatrix}; \tag{4}$$

where $\hat{\mathbf{K}}_M^{ij}$ and $\mathbf{K}_B^i$ are mesh interface and bearing stiffness matrices, respectively. Here $\mathbf{P}$ is a diagonal transformation matrix defined in accordance with the adopted coordinate system and is given by

$$\mathbf{P} = \text{diag}[-1 \quad -1 \quad -1 \quad -1 \quad 1 \quad 1]. \tag{5}$$

The mesh stiffness matrices $\hat{\mathbf{K}}_M^{ij}$ and $\hat{\mathbf{K}}_M^{ji}(5 \times 5)$ are obtained directly from the gear mesh interface model given in Ref. [15] by ignoring the x DOF and are given respectively by

$$\hat{\mathbf{K}}_M^{ij} = K_M \begin{bmatrix} c^2 & & & & \\ cs & s^2 & & \text{sym} & \\ \kappa^{ij}c & \kappa^{ij}s & \mu^{ij} & & \\ -cs & -s^2 & -\kappa^{ij}s & s^2 & \\ c^2 & cs & \kappa^{ij}c & -cs & c^2 \end{bmatrix} \tag{6}$$

and

$$\hat{\mathbf{K}}_M^{ji} = K_M \begin{bmatrix} c^2 & & & & \\ cs & s^2 & & \text{sym} & \\ \kappa^{ji}c & \kappa^{ji}s & \mu^{ji} & & \\ cs & s^2 & \kappa^{ji}s & -s^2 & \\ -c^2 & -cs & -\kappa^{ji}c & cs & -c^2 \end{bmatrix} \tag{7}$$

Here $c = \cos\psi_b$ and $s = \sin\psi_b$ where $\psi_b^i = \psi_b^j = \psi_b$ is the base helix angle of each gear which must be identical. The functional mesh stiffness parameters K_M, κ^{ij} and μ^{ij} are time-invariant forms of those introduced in Ref. [15]. The scalar stiffness parameter K_M represents the average effective translational mesh stiffness along the theoretical line-of-action. The parameter κ^{ij} describes coupling between the bending $-\theta_x^i$ and the torsional $-\theta_z^i$, lateral-y, axial-z and rocking $-\theta_y^i$ DOF due to axial displacement of the effective gear tooth contact zone from the mass centroid of gear i. The dimensionless stiffness parameter μ^{ij} describes the equivalent rotary stiffness associated with the θ_x^i DOF. For an external gear pair having simple cylindrical bodies with the axial position of the mass centroid coincident with the center of the active gear face width, the bounds on κ^{ij} and μ^{ij} are $-1 \leqslant \kappa^{ij} \leqslant 1$ and $0 \leqslant \mu^{ij} \leqslant 1$. In general, $\kappa^{ij} \neq \kappa^{ji}$ and $\mu^{ij} \neq \mu^{ji}$. It is possible to have $\kappa^{ij} > 1$ when the mass centroid of the gear is displaced axially from the center of the active face width. In such cases where $\kappa^{ij} \gg 1$ the rotary stiffness parameter $\mu^{ij} \cong (\kappa^{ij})^2$.

Bearing stiffness matrices $\mathbf{K}_B^i(5 \times 5)$ in (5) describe the combined stiffness of shafting, bearings and housing structures associated with each gear i. Energy-equivalent viscous damping matrices $\mathbf{C}_B^i$ and $\hat{\mathbf{C}}_M^{ij}(5 \times 5)$ are also assumed to account for all dissipative effects occurring within the bearings and gear mesh interface, respectively. Accordingly, the system damping matrix $\mathbf{C}$ (10×10) takes on the form

$$\mathbf{C} = \begin{bmatrix} \hat{\mathbf{C}}_M^{ij} & \mathbf{P}\hat{\mathbf{C}}_M^{ij} \\ \mathbf{P}\hat{\mathbf{C}}_M^{ji} & \hat{\mathbf{C}}_M^{ji} \end{bmatrix} + \begin{bmatrix} [\mathbf{D}^i]^{-1}\mathbf{C}_B^i[\mathbf{D}^i]^{-1} & \mathbf{O} \\ \mathbf{O} & [\mathbf{D}^j]^{-1}\mathbf{C}_B^j[\mathbf{D}^j]^{-1} \end{bmatrix}. \tag{8}$$

All mesh and bearing stiffness and damping properties required by equations (4) and (8) are assumed to be known.

2.1. Generalized forcing vectors

The components of the five dimensional generalized forcing vector $\mathbf{Q}^i(t) = \mathbf{Q}_\delta^{ij}(t) + \mathbf{Q}_{ext}^i(t)$ acting on gear i is written as the sum of $\mathbf{Q}_\delta^{ij}(t)$, which describes the forces and moments acting on gear i as a result of its meshing with gear j, and $\mathbf{Q}_{ext}^i(t)$, which describes any external forces and moments acting directly on gear i. Here $\mathbf{Q}_\delta^{ij}(t)$ arises from so-called transmission error (TE) which may be described by a vector of equivalent translational displacements $\boldsymbol{\delta}_o^{ij}(t) = \{\delta_y^{ij}(t)\ \delta_z^{ij}(t)\ \delta_{\theta_x}^{ij}(t)\ \delta_{\theta_y}^{ij}(t)\ \delta_{\theta_z}^{ij}(t)\}^T$ occurring within the gear mesh interface due to kinematic tooth errors and variation of the instantaneous mesh stiffness under an applied mean load [1]. Here, subscript o denotes that the TE vector is determined from an independent static analysis or by direct measurement under quasi-static conditions [15]. TE vectors $\boldsymbol{\delta}_o^{ij}(t)$ and $\boldsymbol{\delta}_o^{ji}(t)$ are related by $\boldsymbol{\delta}_o^{ji}(t) = \mathbf{P}\boldsymbol{\delta}_o^{ij}(t)$. Expressions for $\mathbf{Q}_\delta^{ij}(t)$ and $\mathbf{Q}_{ext}^i(t)$ are given respectively by

$$\mathbf{Q}_\delta^{ij}(t) = \hat{\mathbf{K}}_M^{ij}\boldsymbol{\delta}_o^{ij}(t) + \hat{\mathbf{C}}_M^{ij}\dot{\boldsymbol{\delta}}_o^{ij}(t) \tag{9}$$

and

$$\mathbf{Q}_{ext}^i(t) = [\mathbf{D}^i]^{-1}\mathbf{F}_{ext}^i(t). \tag{10}$$

The five dimensional external force vector $\mathbf{F}_{ext}^i(t) = \{F_y^i(t)\ F_z^i(t)\ T_x^i(t)\ T_y^i(t)\ T_z^i(t)\}^T$ describes any forces and moments acting on gear i in terms of gear body coordinates X^i, Y^i and Z^i which are not generated as a result of the meshing action.

2.2. Generalized mesh force vector

The vector of generalized dynamic forces and moments $\mathbf{Q}_{mesh}^{ij}(t)$ transmitted via the gear mesh interface and acting on gear i is given by

$$\mathbf{Q}_{mesh}^{ij}(t) = -\hat{\mathbf{K}}_M^{ij}[\mathbf{q}^i(t) + \mathbf{P}\mathbf{q}^j(t) - \boldsymbol{\delta}_o^{ij}(t)] - \hat{\mathbf{C}}_M^{ij}[\dot{\mathbf{q}}^i(t) + \mathbf{P}\dot{\mathbf{q}}^j(t) - \dot{\boldsymbol{\delta}}_o^{ij}(t)] \tag{11}$$

Hence, forces and moments transmitted via the gear mesh interface arise due to TE excitations as well as external forces and moments acting on gears i and j, respectively. The transmitted mesh force vector in terms of gear body coordinates is given by $\mathbf{F}_{mesh}^{ij}(t) = \mathbf{D}^i\mathbf{Q}_{mesh}^{ij}(t)$.

2.3. Dimensionless form

The natural frequency of an equivalent single degree of freedom torsional gear pair model is given by $\omega = \sqrt{K_M/m_{eq}}$ where $m_{eq} = I_z^i I_z^j/(a^{j2}I_z^i + a^{i2}I_z^j)$ is the system equivalent mass. The equation of motion (1) can be written in a dimensionless form by defining a dimensionless time parameter $\tau = \omega t$ and displacement vector $\mathbf{y}^i(\tau) = \mathbf{q}^i(\tau)/|\epsilon_y|$ where $\epsilon_y = \epsilon_y^{ij} = \epsilon_y^{ji}$ is the so-called kinematic transmission error defined along the line-of-action [1]. For any real gear system, $|\epsilon_y|$ will never be zero due to unavoidable manufacturing errors. Accordingly, the system equation of motions in dimensionless form are given by

$$\begin{bmatrix} \mathbf{m}^i & 0 \\ 0 & \mathbf{m}^j \end{bmatrix}\begin{Bmatrix} \mathbf{y}''^i \\ \mathbf{y}''^j \end{Bmatrix} + \mathbf{c}\begin{Bmatrix} \mathbf{y}'^i \\ \mathbf{y}'^j \end{Bmatrix} + \mathbf{k}\begin{Bmatrix} \mathbf{y}^i(\tau) \\ \mathbf{y}^j(\tau) \end{Bmatrix} = \begin{Bmatrix} \mathbf{f}^i(\tau) \\ \mathbf{f}^j(\tau) \end{Bmatrix}. \tag{12}$$

Here $(')$ denotes differentiation with respect to τ and $\mathbf{f}^i(\tau) = \mathbf{Q}^i(\tau)/(K_M|\epsilon_y|) = \mathbf{f}_\delta^{ij}(\tau) + \mathbf{f}_{ext}^i(\tau)$ is a dimensionless forcing vector. The dimensionless mass, damping and stiffness matrices are given respectively by $\mathbf{m}^i = [\mathbf{D}^i]^{-1}\mathbf{M}^i[\mathbf{D}^i]^{-1}/m_{eq}$, $\mathbf{c} = \mathbf{C}/\omega$ and $\mathbf{k} = \mathbf{K}/\omega^2$.

2.4. *Periodicity of excitation functions*

Normally the TE vector $\delta_o^{ij}(t)$ is assumed to be periodic in time t at the gear meshing frequency $N^i\Omega^i$ where N^i is the number of teeth on gear i. Similarly each external forcing vector $\mathbf{F}_{ext}^i(t)$ is assumed to be periodic in t having fundamental frequency Ω_{ext}^i. Accordingly, $\mathbf{f}_\delta^{ij}(\tau)$ and $\mathbf{f}_\delta^{ji}(\tau)$ are periodic in τ with dimensionless fundamental frequency $\Lambda^{ij} = N^i\Omega^i/\omega$ and each $\mathbf{f}_{ext}^i(\tau)$ is periodic with fundamental frequency $\Lambda_{ext}^i = \Omega_{ext}^i/\omega$. Further, $\mathbf{f}(\tau)$ may be expanded in terms of three Fourier series in τ each having fundamental frequency Λ^{ij}, Λ_{ext}^i and Λ_{ext}^j, respectively. In many rotating machinery systems, Λ^{ij}, Λ_{ext}^i and Λ_{ext}^j, are commensurate and $\mathbf{f}(\tau)$ can be expanded in terms of a single Fourier series in τ having some common fundamental frequency, say Λ [1, 15].

3. STEADY-STATE FORCED RESPONSE SOLUTION

Since the steady state forced response of the linear system to harmonic or periodic excitations is of interest, the determination of appropriate frequency response functions is sufficient. Accordingly, dimensionless dynamic compliance matrix $\tilde{\mathbf{H}}(\Lambda)$ is defined such that $\tilde{\mathbf{Y}}(\Lambda) = \tilde{\mathbf{H}}(\Lambda)\tilde{\mathbf{F}}(\Lambda)$ where $\tilde{\mathbf{Y}}(\Lambda)$ and $\tilde{\mathbf{F}}(\Lambda)$ are the Fourier transforms of $\{\mathbf{y}^{iT}(\tau)\,\mathbf{y}^{jT}(\tau)\}^T$ and $\{\mathbf{f}^{iT}(\tau)\,\mathbf{f}^{jT}(\tau)\}^T$, respectively. Here tilde denotes a complex valued quantity. In general, system damping is non-proportional and $\tilde{\mathbf{H}}(\Lambda)$ can be computed in $2N$-space by using the well known modal expansion technique where $N = 10$ system DOF. First the complex eigenvalue problem

$$\tilde{\Lambda}\begin{bmatrix} \mathbf{O} & -\begin{pmatrix} \mathbf{m}^i & 0 \\ 0 & \mathbf{m}^j \end{pmatrix} \\ \begin{pmatrix} \mathbf{m}^i & 0 \\ 0 & \mathbf{m}^j \end{pmatrix} & \mathbf{c} \end{bmatrix}\tilde{\Phi} = -\begin{bmatrix} \begin{pmatrix} \mathbf{m}^i & 0 \\ 0 & \mathbf{m}^j \end{pmatrix} & \mathbf{O} \\ \mathbf{O} & \mathbf{k} \end{bmatrix}\tilde{\Phi} \tag{13}$$

is solved and then $\tilde{\mathbf{H}}(\Lambda)$ is computed by a summation over vibratory modes

$$\tilde{\mathbf{H}}(\Lambda) = \sum_{r=1}^{2N} \frac{\tilde{\Phi}_r^L \tilde{\Phi}_r^{LT}}{j\Lambda - \tilde{\Lambda}_r} = \begin{bmatrix} \tilde{\mathbf{H}}^{ii}(\Lambda) & \tilde{\mathbf{H}}^{ij}(\Lambda) \\ \tilde{\mathbf{H}}^{ji}(\Lambda) & \tilde{\mathbf{H}}^{jj}(\Lambda) \end{bmatrix} \tag{14}$$

where $j = \sqrt{-1}$ and $\tilde{\Phi}_r^L$ is the lower half of the complex eigenvector $\tilde{\Phi}_r$ of dimension $2N$ corresponding to eigenvalue $\tilde{\Lambda}_r$. The eigenvectors are normalized such that

$$\tilde{\Phi}_r^T \begin{bmatrix} \mathbf{O} & -\begin{pmatrix} \mathbf{m}^i & 0 \\ 0 & \mathbf{m}^j \end{pmatrix} \\ \begin{pmatrix} \mathbf{m}^i & 0 \\ 0 & \mathbf{m}^j \end{pmatrix} & \mathbf{c} \end{bmatrix}\tilde{\Phi}_r = 1. \tag{15}$$

The system mass matrix is diagonal and positive definite and the system stiffness matrix is positive semi-definite. There are two rigid body (purely torsional) modes at $\Lambda_r = 0$ which correspond to the intended conjugate action of the gear pair. Equation (12) can be reduced to 9 DOF by combining coordinates $\theta_z^i(t)$ and $\theta_z^j(t)$ to form a single torsional dynamic transmission error (DTE) coordinate $\xi^{ij}(t) = a^i\theta_z^i(t) + a^j\theta_z^j(t)$ and the resulting system stiffness matrix will be positive definite if both ψ_b and μ are non-zero. When either ψ_b or μ are zero, there will be additional rigid body modes and the appropriate DOF can be reduced accordingly.

The complex eigensolution must be employed whenever there are closely spaced modes and/or system damping is heavy. In systems where damping is proportional or modal damping values are less than 10%, a real eigensolution may be employed with sufficient accuracy. In such cases $\tilde{\mathbf{H}}(\Lambda)$ is given by

$$\tilde{\mathbf{H}}(\Lambda) = \sum_{r=1}^{N} \frac{\Phi_r \Phi_r^T}{\Lambda_r^2 - \Lambda^2 + 2j\zeta_r \Lambda\Lambda_r} \tag{16a}$$

where Φ_r is the real eigenvector of dimension N corresponding to real eigenvalue Λ_r obtained by solving the eigenvalue problem

$$\mathbf{k}\Phi = \Lambda^2\begin{pmatrix} \mathbf{m}^i & 0 \\ 0 & \mathbf{m}^j \end{pmatrix}\Phi. \tag{16b}$$

Modal damping ratio ζ_r is given by

$$\zeta_r = \Phi_r^T \mathbf{c} \Phi_r / 2\Lambda_r \tag{16c}$$

with eigenvectors Φ_r normalized according to

$$\Phi_r^T \begin{pmatrix} \mathbf{m}^i & 0 \\ 0 & \mathbf{m}^j \end{pmatrix} \Phi_r = 1. \tag{16d}$$

3.1. Dynamic mesh force

Equation (11) can be written in dimensionless form as follows

$$\mathbf{f}^{ij}_{\text{mesh}}(\tau) = \frac{\mathbf{Q}^{ij}_{\text{mesh}}(\tau)}{K_M |\epsilon_y|} = -\hat{\mathbf{K}}^{ij}_M \left[\mathbf{y}^i(\tau) + \mathbf{P}\mathbf{y}^j(\tau) - \frac{1}{|\epsilon_y|} \boldsymbol{\delta}^{ij}_o(\tau) \right] - \hat{\mathbf{c}}^{ij}_M \left[\mathbf{y}'^i(\tau) + \mathbf{P}\mathbf{y}'^j(\tau) - \frac{1}{|\epsilon_y|} \boldsymbol{\delta}'^{ij}_o(\tau) \right] \tag{17}$$

where $\hat{\mathbf{c}}^{ij}_M = \hat{\mathbf{C}}^{ij}_M / \omega$ and $\hat{\mathbf{k}}^{ij}_M = \hat{\mathbf{K}}^{ij}_M / \omega^2$. This mesh force vector is useful to determine dynamic tooth loading and dynamic stresses and can be expressed in the spectral domain according to

$$\tilde{\mathbf{F}}^{ij}_{\text{mesh}}(\Lambda) = \tilde{\mathbf{G}}^{ij}(\Lambda) \tilde{\boldsymbol{\Delta}}^{ij}(\Lambda) + \tilde{\mathbf{R}}^{ii}(\Lambda) \tilde{\mathbf{F}}^i_{\text{ext}}(\Lambda) + \tilde{\mathbf{R}}^{ij}(\Lambda) \tilde{\mathbf{F}}^j_{\text{ext}}(\Lambda) \tag{18}$$

where $\tilde{\mathbf{F}}^{ij}_{\text{mesh}}(\Lambda)$, $\tilde{\boldsymbol{\Delta}}^{ij}(\Lambda)$ and $\tilde{\mathbf{F}}^i_{\text{ext}}(\Lambda)$ are the dimensionless, complex-valued, Fourier transforms of $\mathbf{f}^{ij}_{\text{mesh}}(\tau)$, $\boldsymbol{\delta}^{ij}_o(\tau)/|\epsilon|$ and $\mathbf{f}^i_{\text{ext}}(\tau)$, respectively. Hence, the generation of forces and moments within the gear mesh interface due to dimensionless transmission error vector $\boldsymbol{\delta}^{ij}_o(\tau)/|\epsilon|$ and acting on gear i is described by the spectral mesh stiffness matrix $\tilde{\mathbf{G}}^{ij}(\Lambda)$ given by

$$\mathbf{G}^{ij}(\Lambda) = \tilde{\mathbf{a}}^{ij}_M - \tilde{\mathbf{a}}^{ij}_M [(\tilde{\mathbf{H}}^{ii} + \mathbf{P}\tilde{\mathbf{H}}^{ji}) \tilde{\mathbf{a}}^{ij}_M + (\tilde{\mathbf{H}}^{ij} + \mathbf{P}\tilde{\mathbf{H}}^{jj}) \tilde{\mathbf{a}}^{jj}_M \mathbf{P}] \tag{19}$$

The above expression may be viewed as a form of multi-dimensional dynamic load factor which may be used by gear designers to de-rate gear load carrying capacity due to dynamic effects. The transmission of external forces via the gear mesh interface and acting on gear i is characterized by the mesh force transmissibility matrix $\tilde{\mathbf{R}}^{ij}(\Lambda)$. Mesh force transmissibility matrices $\tilde{\mathbf{R}}^{ii}(\Lambda)$ and $\tilde{\mathbf{R}}^{ij}(\Lambda)$ (5×5) are given respectively by

$$\tilde{\mathbf{R}}^{ii}(\Lambda) = \tilde{\mathbf{a}}^{ij}_M [\tilde{\mathbf{H}}^{ii} + \mathbf{P}\tilde{\mathbf{H}}^{ji}] \tag{20a}$$

and

$$\tilde{\mathbf{R}}^{ij}(\Lambda) = \tilde{\mathbf{a}}^{ij}_M [\tilde{\mathbf{H}}^{ij} + \mathbf{P}\tilde{\mathbf{H}}^{jj}]. \tag{20b}$$

The complex valued mesh interface stiffness matrix $\tilde{\mathbf{a}}^{ij}_M(\Lambda)$ (5×5) in equations (19) and (20) is given by

$$\tilde{\mathbf{a}}^{ij}_M(\Lambda) = \hat{\mathbf{k}}^{ij}_M + j\Lambda \hat{\mathbf{c}}^{ij}_M. \tag{21}$$

The approach presented in this study is general as it considers two spectral matrices associated with force transmissibility via and force generation within the gear mesh interface, respectively; thus clarifying several issues. Such formulations can also be interpreted within the context of structural finite element programs [3].

3.2. Dynamic bearing force

Similarly, the dimensionless dynamic bearing force vector $\mathbf{f}^{ij}_B(\tau) = [\mathbf{D}^i]^{-1} \mathbf{F}^{ij}_B(\tau) / K_M |\epsilon_y|$ acting on bearing i is given in the spectral domain by

$$\tilde{\mathbf{F}}^{ij}_B(\Lambda) = \tilde{\mathbf{G}}^{ij}_B(\Lambda) \tilde{\boldsymbol{\Delta}}^{ij}(\Lambda) + \tilde{\mathbf{R}}^{ii}_B(\Lambda) \tilde{\mathbf{F}}^i_{\text{ext}}(\Lambda) + \tilde{\mathbf{R}}^{ij}_B(\Lambda) \tilde{\mathbf{F}}^j_{\text{ext}}(\Lambda) \tag{22}$$

where $\tilde{\mathbf{F}}^{ij}_B(\Lambda)$ is the dimensionless, complex-valued, Fourier transform of $\mathbf{f}^{ij}_B(\tau)$. Hence the forces and moments acting on bearing i due to transmission error vector $\boldsymbol{\delta}^{ij}_o(\tau)/|\epsilon|$ is described by the spectral bearing stiffness matrix $\tilde{\mathbf{G}}^{ij}_B(\Lambda)$ given by

$$\tilde{\mathbf{G}}^{ij}_B(\Lambda) = -\tilde{\mathbf{a}}^i_B (\tilde{\mathbf{H}}^{ii} + \mathbf{P}\tilde{\mathbf{H}}^{ij}) \tilde{\mathbf{a}}^{ij}_M \tag{23}$$

The transmission of external forces applied to gear j via the gear mesh interface and acting on bearing i is characterized by the bearing force transmissibility matrix $\tilde{\mathbf{R}}^{ij}_B(\Lambda)$. Bearing force transmissibility matrices $\tilde{\mathbf{R}}^{ii}_B(\Lambda)$ and $\tilde{\mathbf{R}}^{ij}_B(\Lambda)$ (5×5) are given respectively by

$$\tilde{\mathbf{R}}_{\mathrm{B}}^{ii}(\Lambda) = -\tilde{\mathbf{a}}_{\mathrm{B}}^{i}\tilde{\mathbf{H}}^{ii} \tag{24a}$$

and

$$\tilde{\mathbf{R}}_{\mathrm{B}}^{ij}(\Lambda) = -\tilde{\mathbf{a}}_{\mathrm{B}}^{i}\tilde{\mathbf{H}}^{ij}. \tag{24b}$$

The complex valued bearing stiffness matrix $\tilde{\mathbf{a}}_{\mathrm{B}}^{i}(\Lambda)$ (5×5) in equations (23) and (24) is given by

$$\tilde{\mathbf{a}}_{\mathrm{B}}^{i}(\Lambda) = [\mathbf{D}^{i}]^{-1}\mathbf{K}_{\mathrm{B}}^{i}[\mathbf{D}^{i}]^{-1}/\omega^2 + j\Lambda[\mathbf{D}^{i}]^{-1}\mathbf{C}_{\mathrm{B}}^{i}[\mathbf{D}^{i}]^{-1}/\omega \tag{25}$$

3.3. Modal rating indices

It is desirable to develop modal indices which can be used to rank order the importance of gear pair modes excited by various types of TE excitations; especially conventional TE excitations δ_y^{ij} or $\delta_{\theta_z}^{ij}$. Such representations also facilitate the visualization of multi-dimensional, complex-valued vibratory modes; especially those responsible for the generation of gear noise. The gear mesh interface can support only a normal force in the direction of unit vector $\eta^{ij} = \{\sin\psi_{\mathrm{b}}\ \cos\psi_{\mathrm{b}}\ 0\}^{\mathrm{T}}$ and a moment about the X-axis [15]. Accordingly, equivalent modal displacements $\Delta_{\eta r}$ and $\Delta_{\theta_x r}$ are defined in these directions by

$$\Delta_{\theta_x r} = \mathrm{Mod}\{[\cos\psi_{\mathrm{b}}\ \sin\psi_{\mathrm{b}}\ 0\ -\sin\psi_{\mathrm{b}}\ \cos\psi_{\mathrm{b}}]\Delta_r^{\mathrm{U}}\} \tag{26}$$

and

$$\Delta_{\theta_x r} = \mathrm{Mod}\{[0\ 0\ 1\ 0\ 0]\Delta_r^{\mathrm{U}}\} \tag{27}$$

where Δ_r^{U} is the upper half of the relative modal mesh displacement vector Δ_r of dimension $2N$ defined by

$$\Delta_r = \begin{pmatrix} \mathbf{I} & \mathbf{O} \\ \mathbf{O} & \mathbf{O} \end{pmatrix}\tilde{\Phi}_r^{\mathrm{L}} + \begin{pmatrix} \mathbf{O} & \mathbf{P} \\ \mathbf{O} & \mathbf{O} \end{pmatrix}\tilde{\Phi}_r^{\mathrm{L}}. \tag{28}$$

Here $\mathbf{I}$ is the identity matrix. The resultant elastic normal force and moment transmitted by the gear mesh interface associated with each mode r is related to $\Delta_{\eta r}$ and $\Delta_{\theta_x r}$, respectively so long as $\kappa = 0$. Hence by normalizing the $\tilde{\Phi}_r$ such that $\tilde{\Phi}_r^{\mathrm{T}}\tilde{\Phi}_r = 1$, $\Delta_{\eta r}$ may be used to rank order modes which will be excited by δ_y^{ij}, δ_z^{ij}, $\delta_{\theta_y}^{ij}$ and $\delta_{\theta_z}^{ij}$ or by F_y^i, F_z^i, T_y^i, and T_z^i. Similarly, $\Delta_{\theta_x r}$ may be used to rank order modes excited by $\delta_{\theta_x}^{ij}$ or T_x^i. The concepts of $\Delta_{\eta r}$ and $\Delta_{\theta_x r}$ may be extended to large-scale finite element models to determine which modes may be truncated in analyses which attempt to predict gear noise and vibration due to mesh excitations. When $\kappa \neq 0$, the elastic normal force and moment carried by the mesh interface are related to $\Delta_{\eta r} + \kappa\Delta_{\theta_x r}$ and $\kappa\Delta_{\eta r} + \mu\Delta_{\theta_x r}$, respectively. In such cases, it is desirable to quantify the coupling strength between η and θ_x modes. This is accomplished by considering the modal strain energy associated with elastic deflections of the mesh interface. The total mesh interface strain energy U_r is given by

$$U_r = \tilde{\Phi}_r^{\mathrm{T}}\begin{bmatrix} \hat{\mathbf{K}}_{\mathrm{M}}^{ij} & \mathbf{P}\hat{\mathbf{K}}_{\mathrm{M}}^{ij} \\ \mathbf{P}\hat{\mathbf{K}}_{\mathrm{M}}^{ji} & \hat{\mathbf{K}}_{\mathrm{M}}^{ji} \end{bmatrix}\tilde{\Phi}_r = U_{\eta r} + U_{\theta_x r} + U_{\eta\theta_x r} \tag{29}$$

where $U_{\eta r}$ and $U_{\theta_x r}$ represent the strain energy associated with the η and θ_x modes, respectively, and are given by

$$U_{\eta r} = \tfrac{1}{2}\Delta_{\eta r}^2; \quad \text{and} \quad U_{\theta_x r} = \tfrac{1}{2}\Delta_{\theta_x r}^2 \tag{30a,b}$$

The degree of η-θ_x modal coupling due to κ is related to the ratio $|U_{\eta\theta_x r}/(U_{\eta r} + U_{\theta_x r})| \leqslant 1$ for each mode of interest where the coupling strain energy $U_{\eta\theta_x r}$ is given by

$$U_{\eta\theta_x r} = \kappa\Delta_{\eta r}\Delta_{\theta_x r}. \tag{30c}$$

4. REDUCED MODEL: SIMPLE HELICAL GEAR PAIR

In the most general case, the simplified model presented in the previous section requires that 18 independent inertial and mesh stiffness parameters be defined in addition to gear mesh damping values and bearing stiffness and damping matrices. In order to reduce the number of system

parameters so that a meaningful parametric study can be performed here, several simplifying assumptions are made which are quite reasonable for a typical cylindrical body gear pair. A gear pair having $b^i = b^j = b$ with a centralized tooth face such that $\kappa^{ij} = \kappa^{ji} = \kappa$ and $\mu^{ij} = \mu^{ji} = \mu$ is considered. For such a gear, $I_z^i = m^i \rho^{i2}$ and $I_x^i = I_y^i = 0.5 I_z^i$. The mass ratio is assumed to be proportional to the square of the ratio of the base radii; i.e. $m^j/m^i \cong \lambda^{ij2}$. Further, the radius of gyration ρ^i is assumed to be equal to the base radius; i.e. $\rho^i \cong a^i$. Accordingly, the dimensionless mass matrix $\mathbf{m}^i$ is reduced to

$$\mathbf{m}^i = \text{diag}[1 \quad 1 \quad 0.5(v^i)^2 \quad 0.5 \quad 1] \tag{31}$$

where $v^i = a^i/b$ is an aspect ratio with $v^j = v^i \lambda^{ij}$. A dimensionless mesh stiffness matrix (10×10) is defined according to

$$\mathbf{k}_{\mathrm{M}}^{ij} = \frac{1}{K_{\mathrm{M}}} \begin{bmatrix} \hat{\mathbf{K}}_{\mathrm{M}}^{ij} & \mathbf{P}\hat{\mathbf{K}}_{\mathrm{M}}^{ij} \\ \mathbf{P}\hat{\mathbf{K}}_{\mathrm{M}}^{ji} & \hat{\mathbf{K}}_{\mathrm{M}}^{ji} \end{bmatrix} \tag{32a}$$

which is given in its reduced form by

$$\mathbf{k}_{\mathrm{M}}^{ij} = \begin{bmatrix} c^2 & & & & & & & & & \\ cs & s^2 & & & & & & & & \\ \kappa c & \kappa s & \mu & & & & & & & \\ -cs & -s^2 & -\kappa s & s^2 & & & & & & \\ c^2 & cs & \kappa c & -cs & c^2 & & & & & \\ -c^2 & -cs & -\kappa c & cs & -c^2 & c^2 & & & & \\ -cs & -s^2 & -\kappa s & s^2 & -cs & cs & s^2 & & & \\ -\kappa c & -\kappa c & -\mu & \kappa s & -\kappa c & \kappa c & \kappa s & \mu & & \\ -cs & -s^2 & -\kappa s & s^2 & -cs & cs & s^2 & \kappa s & s^2 & \\ c^2 & cs & \kappa c & -cs & c^2 & -c^2 & -cs & -\kappa c & -cs & c^2 \end{bmatrix} \tag{32b}$$

In order to further simplify the problem, bearing stiffness matrices $\mathbf{K}_{\mathrm{B}}^i$ are assumed to be diagonal with $K_{\mathrm{B}\theta_x\theta_x}^i = K_{\mathrm{B}\theta_y\theta_y}^i = K_{\mathrm{B}\theta\theta}^i$ and $K_{\mathrm{B}\theta_z\theta_z}^i = 0$. Bearing stiffness ratios $\alpha_{\mathrm{B}_y}^i = K_{\mathrm{B}yy}^i/K_{\mathrm{M}}$, $\alpha_{\mathrm{B}_z}^i = K_{\mathrm{B}zz}^i/K_{\mathrm{M}}$ and $\alpha_{\mathrm{B}_\theta}^i = K_{\mathrm{B}\theta\theta}^i/K_M a^{i2}$ are defined such that the dimensionless bearing stiffness matrix

$$\mathbf{k}_{\mathrm{B}}^i = ([\mathbf{D}^i]^{-1}\mathbf{K}_{\mathrm{B}}^i[\mathbf{D}^i]^{-1})/K_{\mathrm{M}} \tag{33a}$$

is reduced to

$$\mathbf{k}_{\mathrm{B}}^i = \text{diag}[\alpha_{\mathrm{B}_y}^i \quad \alpha_{\mathrm{B}_z}^i \quad (v^i)^2 \quad \alpha_{\mathrm{B}_\theta}^i \quad \alpha_{\mathrm{B}_\theta}^i \quad 0]. \tag{33b}$$

The dimensionless system stiffness matrix is now given by

$$\mathbf{k} = \left[\mathbf{k}_{\mathrm{M}}^{ij} + \begin{pmatrix} \mathbf{k}_{\mathrm{B}}^i & \mathbf{O} \\ \mathbf{O} & \mathbf{k}_{\mathrm{B}}^j \end{pmatrix}\right]. \tag{34}$$

Hence, the number of parameters required by (12), excluding damping values, is reduced to 11, which is still somewhat unwieldy to perform a fundamental parametric study.

4.1. Special case: unity ratio helical gear pair

For the special case of a unity ratio gear pair ($\lambda^{ij} = 1$) where both gear i and gear j are identical and further, $\mathbf{K}_{\mathrm{B}}^i = \mathbf{K}_{\mathrm{B}}^j$, both $\Delta_{\eta r}$ and $\Delta_{\theta_x r}$ are zero for 5 modes. Consequently, if only force transmission via the gear mesh interface is of interest, equation (12) may be reduced to only 5 functional DOF in terms of the dimensionless dynamic transmission error vector $\mathbf{e}(\tau) = \mathbf{y}^i(\tau) + \mathbf{P}\mathbf{y}^j(\tau)$. The resulting equation of motion is given by

$$\mathbf{m}_\Delta \mathbf{e}''(\tau) + \mathbf{c}_\Delta \mathbf{e}'(\tau) + \mathbf{k}_\Delta \mathbf{e}(\tau) = \mathbf{f}_\Delta(\tau). \tag{35}$$

where $\mathbf{m}_\Delta = \mathbf{m}^i$, $\mathbf{k}_\Delta = 2\hat{\mathbf{k}}_{\mathrm{M}}^{ij} + \mathbf{k}_{\mathrm{B}}^i$, $\mathbf{c}_\Delta = 2\hat{c}_{\mathrm{M}}^{ij} + \mathbf{c}_{\mathrm{B}}^i$ and

$$\mathbf{f}_\Delta(\tau) = \hat{\mathbf{k}}_{\mathrm{M}}^{ij} \delta_o^{ij}(\tau) + (\mathbf{f}_{\mathrm{ext}}^i(\tau) + \mathbf{P}\mathbf{f}_{\mathrm{ext}}^j(\tau)). \tag{36}$$

Accordingly, the reduced spectral mesh $\tilde{\mathbf{G}}_\Delta(\Lambda)$ and bearing $\tilde{\mathbf{G}}_{B\Delta}(\Lambda)$ stiffness matrices (5 × 5) are given respectively by

$$\tilde{\mathbf{G}}_\Delta(\Lambda) = \tilde{\mathbf{a}}_M^{ij} - \tilde{\mathbf{a}}_M^{ij}\tilde{\mathbf{H}}_\Delta(\Lambda)\tilde{\mathbf{a}}_M^{ij} \quad \text{and} \quad \tilde{\mathbf{G}}_{B\Delta}(\Lambda) = -\tilde{\mathbf{a}}_B^{i}\tilde{\mathbf{H}}_\Delta(\Lambda)\hat{\mathbf{a}}_M^{ij} \tag{37a, b}$$

and the reduced mesh $\tilde{\mathbf{R}}_\Delta(\Lambda)$ and bearing $\tilde{\mathbf{R}}_{B\Delta}(\Lambda)$ transmissibility matrices are given respectively by

$$\tilde{\mathbf{R}}_\Delta(\Lambda) = \tilde{\mathbf{a}}_M^{ij}\tilde{\mathbf{H}}_\Delta(\Lambda) \quad \text{and} \quad \tilde{\mathbf{R}}_{B\Delta}(\Lambda) = \tilde{\mathbf{a}}_B^{i}\tilde{\mathbf{H}}_\Delta(\Lambda). \tag{38a, b}$$

If proportional damping is assumed, the corresponding dynamic compliance matrix $\tilde{\mathbf{H}}_\Delta(\Lambda)(5 \times 5)$ can be computed by

$$\tilde{\mathbf{H}}_\Delta(\Lambda) = \sum_{r=1}^{5} \frac{\Phi_r \Phi_r^T}{\Lambda_r^2 - \Lambda^2 + 2j\zeta_r \Lambda \Lambda_r} \tag{39}$$

where Φ_r is the eigenvector corresponding to eigenvalue Λ_r obtained by solving the real eigenvalue problem $\mathbf{k}_\Delta \Phi = \Lambda^2 \mathbf{m}_\Delta \Phi$. Modal damping ratio ζ_r is given by $\zeta_r = \Phi_r^T \mathbf{c}_\Delta \Phi_r / 2\Lambda_r$ and eigenvectors Φ_r are normalized according to $\Phi_r^T \mathbf{m}_\Delta \Phi_r = 1$. Otherwise, $\tilde{\mathbf{H}}_\Delta(\Lambda)$ must be computed by using a reduced form of (14). The reduced system (35) is now described by six dimensionless parameters, excluding damping values, only for the special case when gear i is identical to gear j and $\mathbf{K}_B^i = \mathbf{K}_B^j$. If $\mathbf{K}_B^i \neq \mathbf{K}_B^j$, stiffness coupling will prevent the reduction of (12) to the functional 5 DOF form of (35). Further, if $\mathbf{M}^i \neq \mathbf{M}^j$, both stiffness and inertia coupling make reduction to 5 DOF impossible.

The system of equation (35) is positive definite when both ψ_b and μ are non-zero. The system DOF can be reduced for the spur gear case ($\psi_b = 0$) by deleting the rocking-θ_y and axial-z DOF, and similarly by deleting the bending-θ_x DOF when $\mu = 0$. Accordingly, the reduced system will always be positive definite. This latter case will yield a simple two DOF spur gear model having only torsional and lateral motions. In the case of a non-unity ratio spur gear pair, the above assumptions will yield a three DOF model; such models pervade the gear dynamics literature [1]. Accordingly, the two DOF spur gear model having $\mu = 0$ and $\psi_b = 0$ is chosen as a benchmark.

5. EXAMPLE STUDIES

Some example studies are performed using the reduced model of Section 4.1 to demonstrate the significance of $\tilde{\mathbf{R}}_\Delta(\Lambda)$ and its sensitivity to parameters ψ_b, κ, μ and α. Similar trends exist for $\tilde{\mathbf{G}}_\Delta(\Lambda)$. In practice, the bearing stiffness matrix $\mathbf{K}_B^i$ will rarely be diagonal for most geared systems [16]. This assumption was made only so that the example system could be characterized by a minimum number of parameters. Demonstrating that coupling terms of $\tilde{\mathbf{R}}_\Delta(\Lambda)$ and $\tilde{\mathbf{G}}_\Delta(\Lambda)$ are significant is sufficient to conclude that additional coupling terms must also be included in structure borne noise models where $\tilde{\mathbf{G}}_{B\Delta}(\Lambda)$ and $\tilde{\mathbf{R}}_{B\Delta}(\Lambda)$ are critical.

Physical gear data are provided in Table 1 and the corresponding dimensionless gear parameters are listed in Table 2. In order to facilitate the analysis, uniform modal damping is assumed with $\zeta_r = 0.04$. Parameters values $\alpha_{By} = 2.0$, $\kappa = 0.5$ and $\mu_{max} = \kappa^2 - \frac{1}{3}(1 - |\kappa|)^2$ are used unless otherwise specified. Modal indices r are in order of decreasing frequency and in all cases $\Delta_{\eta r}$ and $\Delta_{\theta_x r}$ have been normalized so that their respective maximum values are unity for all modes.

Table 1. Physical data for example gear system

Dimensional helical gear parameters	
Number of teeth:	N = 50
Normal module:	= 3.0
Pressure angle:	= 20°
Helix angle:	ψ_b = 0–30°
Base radius:	a = 70.48 mm
Face width:	b = 21.14 mm
Mass:	m = 2.882 kg
Radius of gyration:	ρ = 70.48 mm
Average mesh stiffness:	$K_M = 3.00 \times 10^8$ N/m
System natural frequency:	ω = 10203.7 rad/s
Radial stiffness:	$K_{Byy} = 6.00 \times 10^8$ N/m
Axial stiffness:	$K_{Bzz} = 1.50 \times 10^8$ N/m
Bending stiffness:	$K_{B\theta\theta} = 6.71 \times 10^8$ N-m/rad

Table 2. Dimensionless parameters for example gear system

Dimensionless helical gear parameters	
Gear ratio:	$\lambda = 1$
Aspect ratio:	$\nu = 0.3$
Bearing stiffness ratios:	
Radial:	$\alpha_{B_y} = 2.0$
Axial:	$\alpha_{B_z} = 0.5$
Bending:	$\alpha_{B_\theta} = 0.4$
Gear mesh stiffness parameters:	
Translational–rotational:	$\kappa = 0.5$
Rotational–rotational:	$\mu = 0.333$

5.1. Benchmark example: 2 DOF spur gear pair

The spur gear case ($\psi_b = 0°$) is considered first with both $\kappa = 0$ and $\mu = 0$. Only two modes are of interest: torsional-θ_z and lateral-y. Bending-θ_x, rocking-θ_y and axial-z modes do not contribute to $\Delta_{\eta r}$ under these conditions and $\Delta_{\theta_x r} = 0$. In most parallel axis gear pairs $\alpha_{B_y} > 0.1$ and the system is characterized by mode shapes similar to those shown in Fig. 2 given $\alpha_{B_y} = 2.0$. In order to clearly define the dynamic behavior, a few new terms are defined. Any mode having $\Delta_{\eta r} = 1$ or $\Delta_{\theta_x r} = 1$ is denoted as a *primary* normal or bending mesh mode, respectively. All other modes having non-zero $\Delta_{\eta r}$ or $\Delta_{\theta_x r}$ are denoted as *secondary* normal or bending mesh modes, respectively.

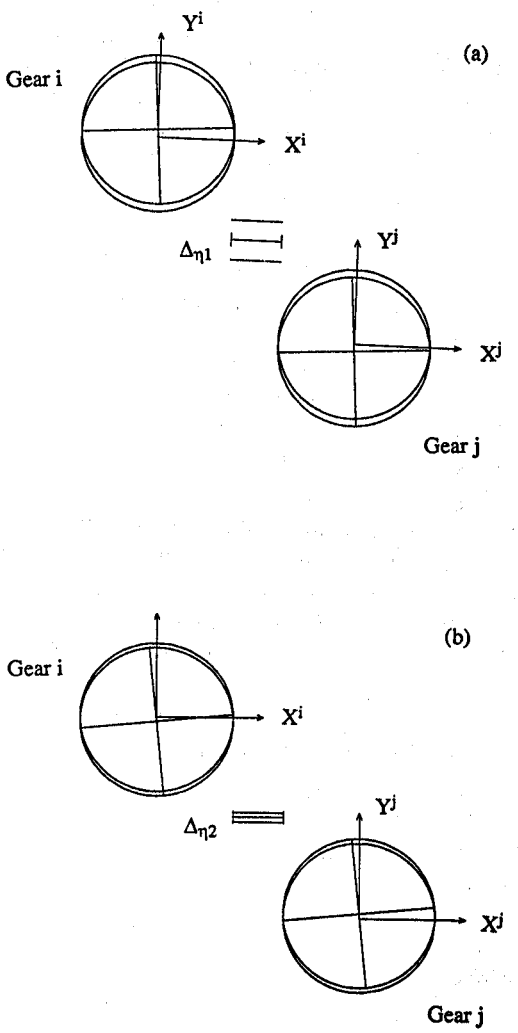

Fig. 2. Typical spur gear pair mesh mode shapes: (a) primary mesh mode ($r = 1$) with $\Lambda_1 = 1.61803$ and $\Delta_{\eta 1} = 1$; (b) secondary mesh mode ($r = 2$) with $\Lambda_2 = 0.61803$ and $\Delta_{\eta 2} = 0.23067$.

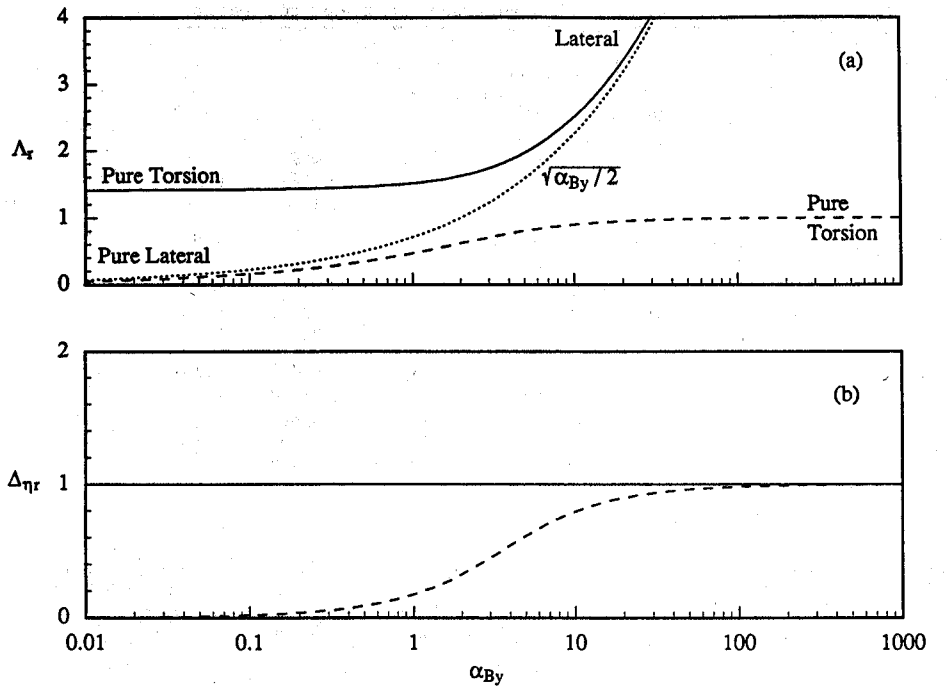

Fig. 3. Influence of bearing flexibility on spur gear modes: (a) Λ_1(——) and Λ_2(– – –) versus α_{B_y}; (b) $\Delta_{\eta 1}$(——) and $\Delta_{\eta 2}$(– – –) versus α_{B_y}.

In the example case shown in Fig. 2, torsional and lateral displacements add directly to form a primary mesh mode ($\Delta_{\eta 1} = 1$) at $\Lambda_1 = 1.61803$. However, the $r = 2$ modal displacements θ_z and y tend to cancel, thus diminishing the combined relative normal mesh displacement $\Delta_{\eta 2} = 0.23607$ creating a secondary mesh mode at $\Lambda_2 = 0.61803$. The eigenvalues Λ_1 and Λ_2 are dictated entirely by bearing stiffness ratio α_{B_y} as shown in Fig. 3(a). A purely torsional model predicts a single mode at $\Lambda_1 = 1$. The effect of bearing flexibility is always to increase $\Lambda_1 \geqslant \sqrt{2}$. As $\alpha_{B_y} \to \infty$, $\Lambda_1 \to \sqrt{\alpha_{B_y}/2}$ and $\Lambda_2 \to 1$. The corresponding ($r = 1$) mode shape becomes purely torsional and the ($r = 2$) mode becomes a purely lateral or bouncing mode. Both $\Delta_{\eta 1}$ and $\Delta_{\eta 2}$ approach unity as $\alpha_{B_y} \to \infty$ as shown in Fig. 3(b). Hence, it is possible to have more than one primary mesh mode. However, when the gear pair is supported by rigid (or very stiff) bearings, only the purely torsional primary mesh mode is of interest. The other primary mesh mode will always be associated with purely lateral motion and has no practical significance since the corresponding natural frequency will approach infinity. There can only be one primary bending mode in models which include the θ_x DOF.

In general, both $\tilde{\mathbf{G}}_\Delta(\Lambda)$ and $\tilde{\mathbf{R}}_\Delta(\Lambda)$ are symmetric matrices with $\tilde{R}_{\Delta\theta_z y} = \tilde{R}_{\Delta\theta_z y}$ and $\tilde{G}_{\Delta\theta_z\theta_z} = \tilde{G}_{\Delta\theta_z y} = \tilde{G}_{\Delta yy}$. The term $\tilde{G}_{\Delta\theta_z y}(\Lambda) - \tilde{a}^{ij}_{M\theta_z y}$ corresponds to the forced response (torsional dynamic transmission error versus Λ) arising from harmonic δ_y type transmission error excitations. This term is the one considered by most investigators and is known as a dynamic load factor. Indeed the amplitude $|\tilde{G}_{\Delta\theta_z y}(\Lambda) - \tilde{a}^{ij}_{M\theta_z y}|$ is significantly larger when Λ is near the primary resonance Λ_1 compared with its amplitude near $\Lambda \cong \Lambda_2$ given $\zeta_2 = \zeta_1$ as shown in Fig. 4. The predominately torsional mode will always produce a larger amplitude in this forced response curve. The corresponding force transmissibility terms $\tilde{R}_{\Delta\theta_z y} = \tilde{R}_{\Delta\theta_z\theta_z}$ do not behave in an identical fashion. In most cases, the secondary resonant amplitude will be equal to or greater than the primary resonant amplitude so long as $\zeta_1 \cong \zeta_2$. The amplitude of $\tilde{R}_{\Delta yy}$ is also shown in Fig. 4 for comparison. The above behavior is characteristic of a unity ratio spur gear pair. Similar trends exist for non-unity ratio spur gear pairs, although two distinct secondary mesh modes exist given $m^i \neq m^j$ or $\alpha^i_{B_y} \neq \alpha^j_{B_y}$.

5.2. Axial and rocking force transmissibility

In order to illustrate axial and rocking force transmissibility, the case $\kappa = 0$ is considered with $0° \leqslant \psi_b \leqslant 40°$. When $\kappa = 0$, no coupling exists between bending-θ_x ($r = 3$) and other modes. Consequently, $U_{\eta\theta_x r} = 0$ for all modes as listed in Tables 3(a) and 3(b). When $\psi_b = 0$ (spur gear),

Table 3. Influence of mesh parameters ψ_b, κ and μ on the modal properties of a simple unity ratio helical gear pair

Case	r	Mode description	Λ_r	$\Lambda_{\eta r}$	$\Delta_{\theta_x r}$	$\dfrac{U_{\eta\theta_x r}}{U_{\eta r}+U_{\theta_x r}}$
(*a*) *Spur gear*	1	Primary normal $(y-\theta_z)$	1.61803	1.0000	0.0000	0.0000
$\psi_b=0$	2	Secondary normal (θ_z-y)	0.61803	0.2361	0.0000	0.0000
$\kappa=0$	3	Primary bending (θ_x)	0.45321	0.0000	1.0000	0.0000
$\mu=0.3333$	4	Pure rocking (θ_y)	0.44721	0.0000	0.0000	0.0000
	5	Pure axial (z)	0.35355	0.0000	0.0000	0.0000
(*b*) *Helical gear*	1	Primary normal $(y-\theta_z-\theta_y-z)$	1.65347	1.0000	0.0000	0.0000
$\psi_b=30$	2	Coupled $(y-\theta_z-\theta_y-z)$	0.78343	0.1975	0.0000	0.0000
$\kappa=0$	3	Primary bending (θ_x)	0.45321	0.0000	1.0000	0.0000
$\mu=0.3333$	4	Coupled $(\theta_y-z-\theta_z-y)$	0.39410	0.0260	0.0000	0.0000
	5	Coupled $(z-\theta_y-\theta_z-y)$	0.26822	0.0428	0.0000	0.0000
(*c*) *Helical gear*	1	Primary normal $(y-\theta_z-\theta_y-z-\theta_x)$	1.65451	1.0000	0.0061	0.0606
$\psi_b=30$	2	Coupled $(y-\theta_z-\theta_y-z-\theta_x)$	0.78400	0.1956	0.0074	0.1598
$\kappa=0.5$	3	Primary bending $(\theta_x-\theta_y-\theta_z-y-z)$	0.44871	0.2628	1.0000	0.8575
$\mu=0.3333$	4	Coupled $(\theta_y-z-\theta_z-y-\theta_x)$	0.39390	0.0282	0.0089	0.0198
	5	Coupled $(z-\theta_y-\theta_z-y-\theta_x)$	0.26800	0.0442	0.0051	0.0032

the axial ($r=5$) and rocking ($r=4$) modes are completely uncoupled and thus cannot be excited by δ_y. Consequently $\Delta_{\eta 4}=0$ and $\Delta_{\eta 5}=0$ as shown in Table 3(a). In this case, eigenvalues Λ_4 and Λ_5 are dictated solely by $\alpha_{B\theta}$ and α_{Bz}, respectively. When $\psi_b\neq 0$ (helical gear), all modes, except the ($r=3$) bending mode, are coupled as evident by the non-zero $\Delta_{\eta r\neq 3}$ values listed in Table 3(b). However, the corresponding eigenvalues are influenced only slightly by ψ_b as shown in Fig. 5. The conventional forced response $|\tilde{G}_{\Delta\theta_z y}(\Lambda)-\tilde{a}^{ij}_{M\theta_z y}|$ versus Λ is shown in Fig. 6 for a range of ψ_b values. The main effect of ψ_b is to increase both the primary ($r=1$) and secondary ($r=2$) resonant frequencies while attenuating their amplitudes by a factor of approx. $\cos^2(\psi_b)$. The ($r=4$) and ($r=5$) resonant amplitudes are relatively small compared with the primary mesh resonance and can therefore be neglected in many cases. This has prompted some investigators to completely ignore the axial and rocking DOF in helical gear pair models [1]. In such cases, an equivalent spur gear model is considered with the corresponding average mesh stiffness adjusted accordingly. The amplitudes of conventional force transmissibility terms $\tilde{R}_{yy}$ and $\tilde{R}_{\theta_z\theta_z}=\tilde{R}_{\Delta\theta_z y}$ are shown in Fig. 7 given $\psi_b=30°$. Note the large resonance in the $\tilde{R}_{\theta_z\theta_z}$ and $\tilde{R}_{\Delta\theta_z y}$ terms near $\Lambda=\Lambda_5$ which is not present given $\psi_b=0°$. Amplitudes of axial terms $\tilde{R}_{\Delta zz}$, $\tilde{R}_{\Delta zy}$ and $\tilde{R}_{\Delta z\theta_z}$ and rocking terms $\tilde{R}_{\Delta\theta_y\theta_y}$, $\tilde{R}_{\Delta\theta_y\theta_z}$,

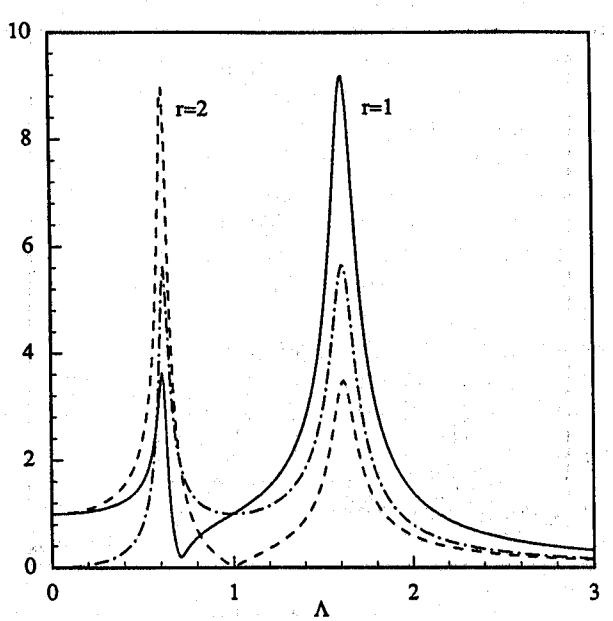

Fig. 4. Typical frequency response curves for a spur gear pair: $|\tilde{G}_{\Delta\theta_z y}-\tilde{a}^{ij}_{M\theta_z y}|$(——), $|\tilde{R}_{\Delta\theta_z y}|=|\tilde{R}_{\Delta\theta_z\theta_z}|$(– – – –) and $|\tilde{R}_{\Delta yy}|$(– · – ·) versus Λ.

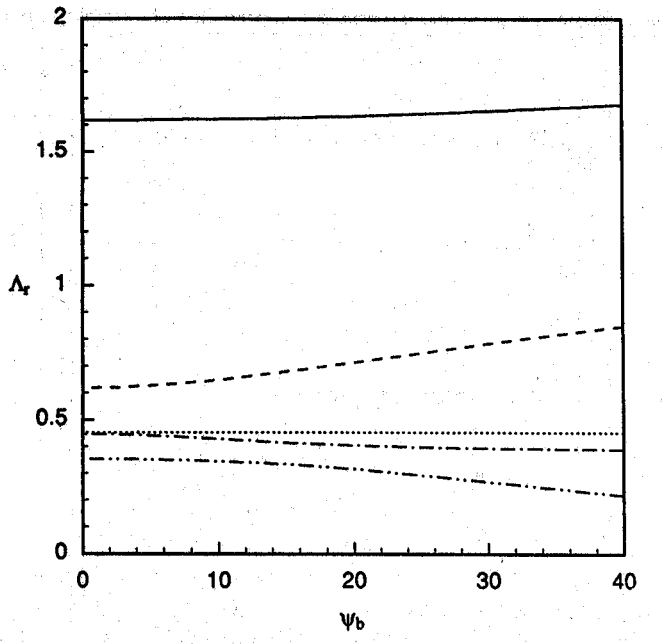

Fig. 5. Influence of helix angle on eigenvalues Λ_r given $\kappa = 0$: Λ_1(——), Λ_2(– – –), Λ_3(· · · ·), Λ_4(– · –) and Λ_5(– · · – · ·) versus ψ_b.

$\tilde{\mathbf{R}}_{\Delta\theta_y y}$ and $\tilde{\mathbf{R}}_{\Delta\theta_y z}$ are shown in Figs 8 and 9, respectively given $\psi_b = 30°$. None of these terms are negligible given non-zero ψ_b.

5.3. *Effect of η–θ_x coupling*

Until now only $\kappa = 0$ has been considered with no coupling between ($r = 3$) bending-θ_x and other modes. When $\kappa \neq 0$ and $\psi_b \neq 0$ coupling exists between all five modes as evident from the non-zero $\Delta_{\eta r}$, $\Delta_{\theta_x r}$ and $U_{\eta\theta_x r}$ values listed in Table 3(c). Given $\mu = \mu_{max}$, κ has only a minor influence on the system eigenvalues as shown in Fig. 10. Since most gear pairs cannot support a mesh frequency harmonic displacement excitation of type $\delta_{\theta x}$, the θ_x DOF has traditionally been ignored [4–10].

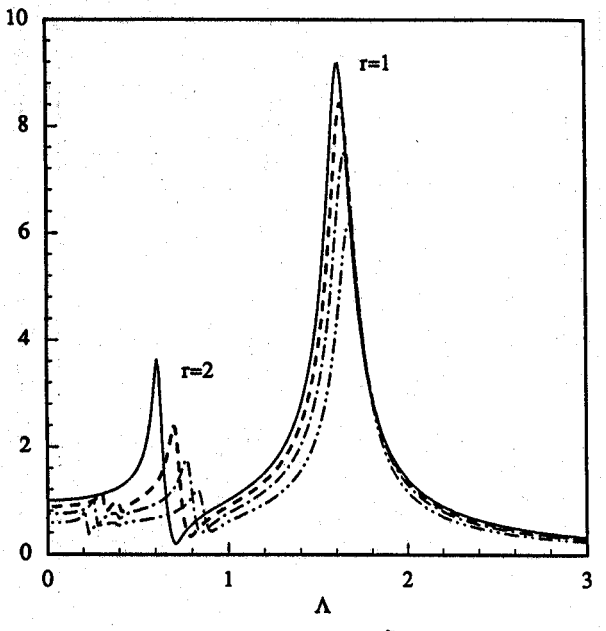

Fig. 6. Conventional forced response of a helical gear pair $|\tilde{G}_{\Delta\theta_z z} - \tilde{a}^{ij}_{M\theta_z y}|$ versus Λ given $\psi_b = 0°$ (——), $\psi_b = 20°$ (– – – –), $\psi_b = 30°$ (– · –) and $\psi_b = 40°$ (– · · – · ·). Refer to Table 3(b) for corresponding Λ_r values.

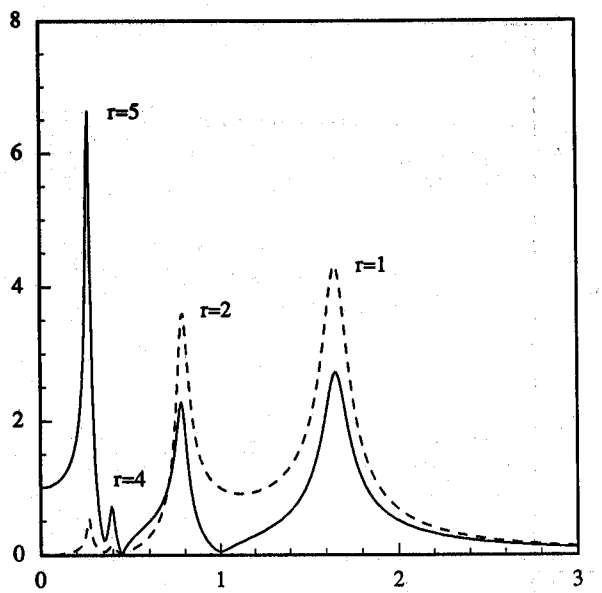

Fig. 7. Conventional mesh force transmissibility terms for a helical gear pair given $\psi_b = 30°$ and $\kappa = 0$: $|\tilde{R}_{\Delta\theta_z y}| = |\tilde{R}_{\Delta\theta_z\theta_z}|$ (——) and $|\tilde{R}_{\Delta yy}|$ (– – – –) versus Λ. Refer to Table 3(b) for corresponding Λ_r values.

However, coupling between η and θ_x DOF will produce bending moments in the transmitted gear mesh force vector. The degree of η–θ_x coupling is dictated by κ and can be characterized by the mesh strain energy ratio $|U_{\eta\theta_x r}/(U_{\eta r} + U_{\theta_x r})|$ which is plotted against κ in Fig. 11 for modes ($r = 1$) through ($r = 5$). The highest degree of η–θ_x coupling is associated with the predominately bending mode ($r = 3$). Amplitudes of the four coupled θ_x force transmissibility terms are shown in Fig. 12 given $\kappa = 0.5$ and $\psi_b = 30°$. The terms $\tilde{R}_{\theta_x y}$ and $\tilde{R}_{\theta_x\theta_z}$ are indeed significant regardless of ψ_b and terms $\tilde{R}_{\theta_x z}$ and $\tilde{R}_{\theta_x\theta_y}$ are significant given non-zero ψ_b. Although not shown, κ also has some influence on the non-θ_x terms of $\tilde{\mathbf{G}}_\Delta(\Lambda)$ and $\tilde{\mathbf{R}}_\Delta(\Lambda)$.

5.4. Summary of gear mesh force transmissibility

Typically, researchers concerned with the forced response of gear pairs have concentrated mostly on $\tilde{G}_{\theta_z y}$ and $\tilde{G}_{yy}$ terms which respectively describe torsional moment and line-of-action force arising

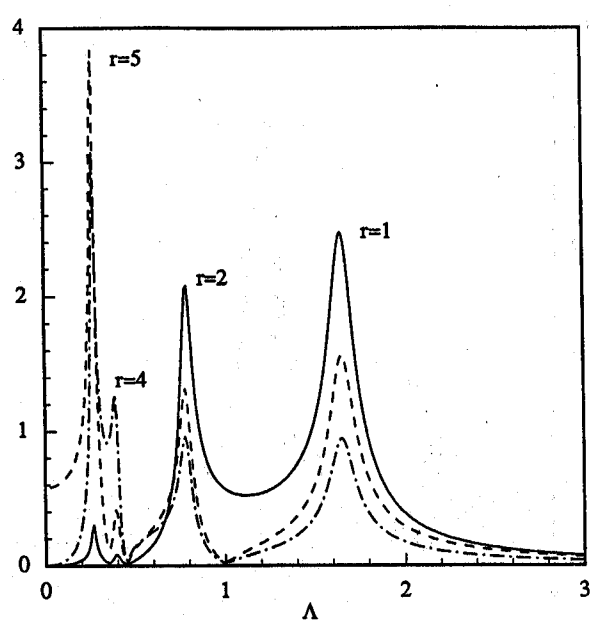

Fig. 8. Axial mesh force transmissibility terms for a helical gear pair given $\psi_b = 30°$ and $\kappa = 0$: $|\tilde{R}_{\Delta z y}|$ (——), $|\tilde{R}_{\Delta z\theta_z}|$ (– – – –) and $|\tilde{R}_{\Delta zz}|$ (– · – ·) versus Λ. Refer to Table 3(b) for corresponding Λ_r values.

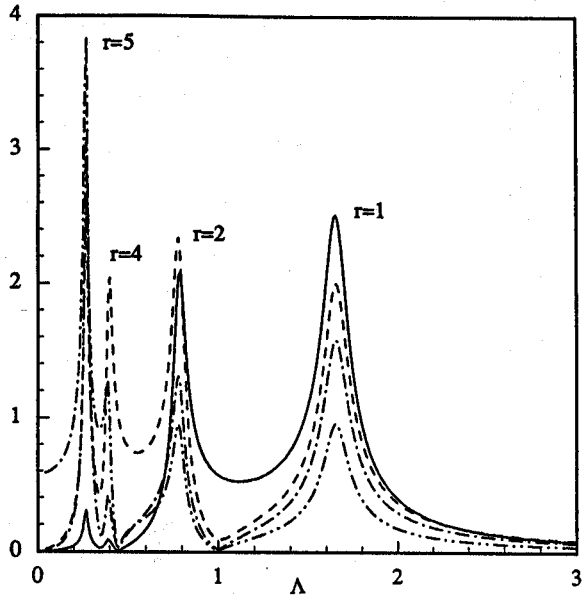

Fig. 9. Rocking mesh force transmissibility terms for a helical gear pair given $\psi_b = 30°$ and $\kappa = 0$: $|\tilde{R}_{\Delta\theta_y y}|$ (——), $|\tilde{R}_{\Delta\theta_y\theta_y}|$ (– – –), $|\tilde{R}_{\Delta\theta_y\theta_z}|$ (– · –) and $|\tilde{R}_{\Delta\theta_y z}|$ (– · · · –) versus Λ. Refer to Table 3(b) for corresponding Λ_r values.

from δ_y type TE excitations. Since these terms are only slightly affected by gear helix angle ψ_b and mesh stiffness coupling parameters κ and μ, the corresponding axial, bending and rocking DOF have traditionally been neglected. However, the above examples clearly illustrate that when gear mesh or bearing force transmissibility is of interest, these DOF must be included in the gear mesh interface model. Of special importance is the coupling between torsional and lateral, axial, bending and rocking DOF. All of these coupling terms, with the exception of y–θ_z terms, are usually assumed to be zero. However, the axial force and rocking and bending moments, arising from external torque fluctuations not generated due to the meshing action, are critical in any analysis which attempts to predict structure borne noise and casing vibration associated with geared rotating machinery.

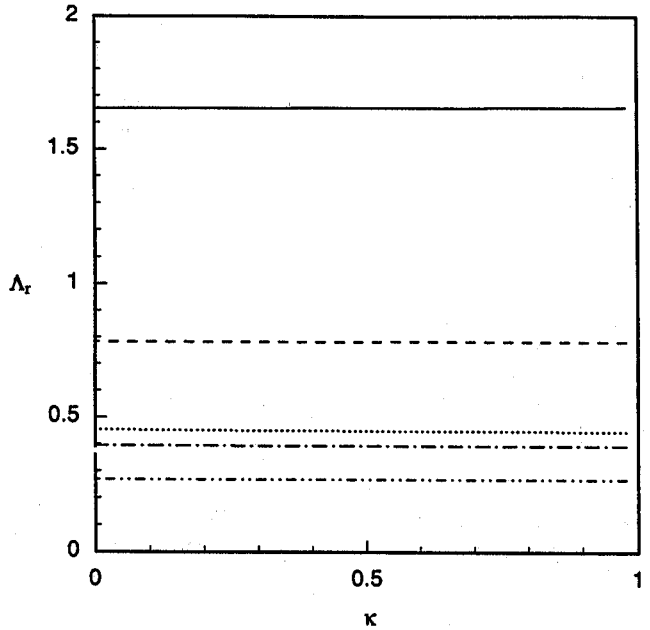

Fig. 10. Influence of κ on helical gear pair eigenvalues Λ_r given $\psi_b = 30°$: Λ_1(——), Λ_2(– – –), Λ_3(· · ·), Λ_4(– · –) and Λ_5(– · · · –) versus κ.

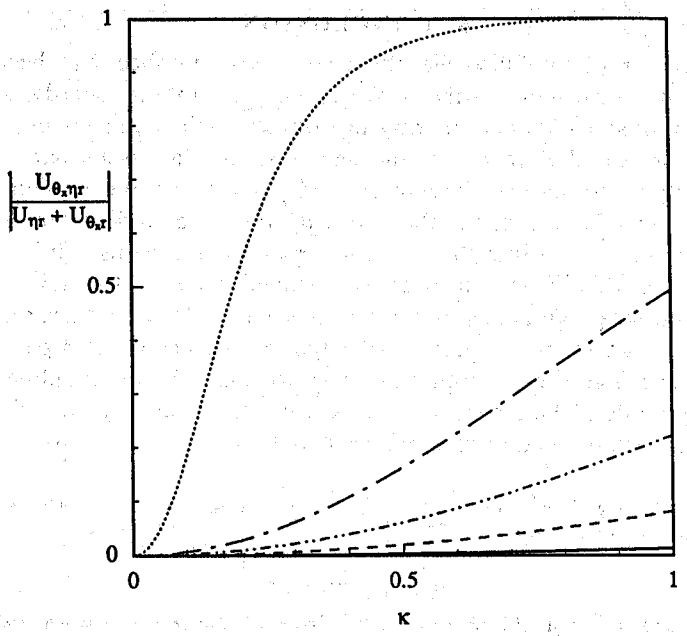

Fig. 11. Influence of κ on $\eta - \theta_x$ modal coupling $|U_{\theta_x\eta r}/(U_{\eta r} + U_{\theta_x r})|$ versus κ given $\psi_b = 30°$ and $r = 1$(——); $r = 2$(– – – –); $r = 3$(· · · ·); $r = 4$(– · – · ·); $r = 5$(– · · – · · ·).

In general, reduction of equation (12) to the 5 DOF form of (35) is not possible and 9 distinct vibratory modes will contribute to the forced response making analytical predictions considerably more complex. Further, overall system characterization is very difficult due to the large number of parameters required to describe the gear-bearing system. However, an accurate description of mesh or bearing force transmissibility still requires the inclusion of the additional DOF in the gear mesh interface model. In cases where $\kappa \gg 1$, coupling associated with shaft flexure will be more significant than that illustrated in Section 5.3. Further, off-diagonal bearing stiffness terms will contribute to force coupling; the relative importance of these terms depends upon the actual physical gear and bearing configurations.

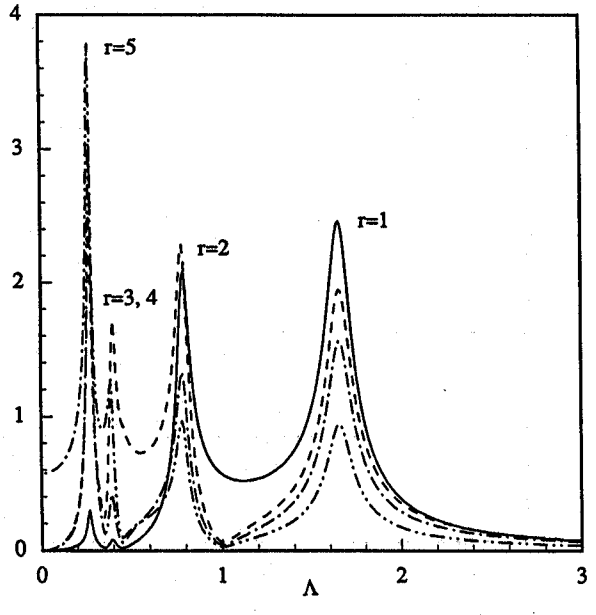

Fig. 12. Bending mesh force transmissibility terms for a helical gear pair given $\psi_b = 30°$ and $\kappa = 0.5$: $|\tilde{R}_{\Delta\theta_x y}|$ (——), $|\tilde{R}_{\Delta\theta_x\theta_y}|$ (– – –), $|\tilde{R}_{\Delta\theta_x\theta_z}|$ (– · – · ·) and $|\tilde{R}_{\Delta\theta_x z}|$ (– · · – · · ·) versus Λ. Refer to Table 3(c) for corresponding Λ_r values.

6. CONCLUSION

The issue of force transmissibility via the gear mesh interface has been clarified. Other investigators have concentrated primarily on vibratory gear motions and dynamic tooth stresses arising from conventional line-of-action transmission error displacement excitation. The transmission of external forces and moments via the gear mesh interface is a separate but related issue. The new model clearly illustrates that these forces and moments are indeed significant and further, that additional DOF must be included in the gear mesh interface model in analyses which attempt to predict the transmission of forces through complex geared systems. The concepts of spectral force transmissibility and stiffness matrices are defined only in the LTI case and may be incorporated into large scale modal analyses of geared systems. New modal rating indices have also been developed which can be used to rank order the importance of gear pair modes excited by various types of transmission error excitations and to quantify the coupling strength between normal and bending modes. These concepts extend to linear time varying and nonlinear cases as well where such effects will have additional influence on mesh force generation and transmissibility.

Acknowledgement—The authors wish to thank the Powertrain Division of General Motors Corporation and Mr Adolph Sbihli of GM Gear Center for supporting this research.

REFERENCES

1. G. W. Blankenship and R. Singh, *ASME Proc. of the Sixth Int. Power Transmission and Gearing Conf.* Paper PGT-92-ABS-093 (1992).
2. T. C. Lim and R. Singh, NASA Contractor Report 185148.
3. M. G. Donley, T. C. Lim and G. C. Steyer, Society of Automotive Engineers, Paper 920762 (1992).
4. A. Kahraman, *J. Vibr. Acoustics, Trans. ASME* **115**, 33–39 (1992).
5. A. Kubo and S. Kiyono, *Bull. Jap. Soc. Mech. Engnrs* **23**, 1536–1543 (1980).
6. S. Kiyono, T. Aida and Y. Fujii, *Bull. Jap. Soc. Mech. Engnrs* **21**, 915–922 (1978).
7. F. Kücükay, *Proc. of the Third Int. Conf. on Vibrations in Rotating Machinery*, Institution of Mechanical Engineers, 81–90 (1984).
8. S. V. Neriya, R. B. Bhat and T. S. Sankar, *ASME J. Vibr. Acoustics, Stress Reliability in Design* **110**, 501–506 (1988).
9. K. Umezawa, American Society of Mechanical Engineers, Paper 84-DET-159 (1984).
10. K. Umezawa, T. Suzuki and T. Sato, *Bull. Jap. Soc. Mech. Engnrs* **29**, 1605–1611 (1986).
11. A. Kubo, *J. Mech. Design, Trans. ASME* **100**, 77–84 (1978).
12. S. Kiyono, Y. Fujii and Y. Suzuki, *Bull. Jap. Soc. Mech. Engnrs* **21**, 923–930 (1981).
13. K. Umezawa, T. Suzuki and H. Houjoh, *Bull. Jap. Soc. Mech. Engnrs* **31**(3), 598–605 (1988).
14. D. Seager, American Society of Mechanical Engineers Paper 69-VIBR-16 (1969).
15. G. W. Blankenship and R. Singh, *Mech. Mach. Theory* **30**, 43–57 (1995).
16. T. A. Harris, *Rolling Bearing Analysis*, Third edition. Wiley, New York (1991).